

The Knight field and the local nuclear dipole-dipole field in an (In,Ga)As quantum dot ensemble

T. Auer*, R. Oulton†, A. Bauschulte, D. R. Yakovlev‡, and M. Bayer
Experimentelle Physik II, Technische Universität Dortmund, 44221 Dortmund, Germany

S. Yu. Verbin, R. V. Cherbunin
Institute of Physics, St. Petersburg State University, St. Petersburg 198504, Russia

D. Reuter and A. D. Wieck
Angewandte Festkörperphysik, Ruhr-Universität Bochum, 44780 Bochum, Germany
(Dated: February 6, 2020)

We present an investigation of the electron-nuclear spin system of negatively doped (In,Ga)As quantum dots (QDs) in millitesla transverse and longitudinal magnetic fields, with the aim of determining the maximum nuclear polarization theoretically achievable in our QD system. The essential parameters governing maximum polarization are determined, namely the nuclear dipole-dipole field and the Knight field of the resident electron. Using these measured quantities, the maximum nuclear field which may be generated is calculated. It is estimated that the relation between the dipole-dipole field and the Knight field allows a nuclear field between 4-7.9 Tesla to build up. In addition, careful measurements of dynamic nuclear polarization in millitesla fields shows a clear demonstration that even very small millitesla fields may have a profound effect on the electron-nuclear dynamics. In particular, we demonstrate that the Hanle effect, typically used to determine electron spin coherence times, may not be used in QD systems to measure spin coherence times greater than ≈ 1 ns, due to the fact that millitesla magnetic fields are screened by the nuclei.

PACS numbers: 42.25.Kb, 78.55.Cr, 78.67.Hc

I. INTRODUCTION

The expectation that the electron spin in semiconductor quantum dots could serve as a building block for quantum computing applications has drawn renewed attention to the role of the quantum dot nuclei. In the seventies it was already shown that for bulk semiconductors, the interplay between an electron spin (at that time, of a donor trapped electron) and the entirety of the nuclear spins in its vicinity leads to a wide variety of effects and often exhibits initially unexpected behavior [1, 2, 3, 4, 5, 6, 7, 8]. In quantum dots the hyperfine coupling between electron and nuclear spins is further enhanced by the localization of the electron in the dot.

Nuclei can be polarized by transfer of angular momentum from optically oriented electrons, known as Overhauser effect [1, 10, 11, 12, 13]. It was shown that nuclear polarization obtained in this way leads to an effective magnetic field of the order Tesla in the quantum dot [11, 14, 15]. Most of these experiments exploited the Overhauser energy shift [16] of the electron Zeeman levels split in an external field where the nuclear field was of the same order of magnitude as the external field. The steady-state nuclear polarization achievable is governed by competition between the rate of angular momentum transfer from the electrons to the nuclei, and the rate of nuclear depolarization. At zero applied field, nuclear depolarization is dominated by the dipole-dipole interaction between the nucleus and its nearest-neighbors [7, 17]. As the time of the dipole-dipole depolarizing interaction is $\approx 10^{-4}$ s at 0 T, two orders of magnitude smaller than the

time the nuclear spins need to become polarized ($\approx 10^{-2}$ s as shown in [18]), no nuclear polarization should occur. In order to obtain nuclear polarization, a magnetic field should be applied to slow down the spin relaxation in the nuclear spin system. The field value should be either much larger than the dipole-dipole field $B_L \approx 0.1$ mT or comparable to it [7]. It was therefore thought that an external magnetic field is required in order to obtain nuclear polarization. It is known now, however, that nuclear polarization also may occur in the absence of an external field [15, 19]. This is possible because spin polarized electrons exert an effective magnetic field, the Knight field B_e [20], on the quantum dot nuclei [7, 8, 9, 19]. The relationship between the magnitude of B_e and the dipole-dipole field B_L determines how efficiently the nuclear spins can be polarized at zero external magnetic field. In order to estimate the nuclear polarization which can be obtained when no external field is present it is therefore necessary to know the magnitude of both the Knight field and the dipole-dipole field.

This is also important concerning the relaxation time of the electron spin in quantum dots which is a decisive quantity for the application of the electron spin in quantum computing: While earlier the fact that the interaction with the nuclei limits the spin relaxation time of the electron was to the fore [21, 22], it was shown recently that the nuclei can, when polarized, in contrary stabilize the electron spin so that under ideal conditions a spin memory is still present after hundreds of milliseconds [23, 24, 25].

In this paper we report experimental studies of

(In,Ga)As quantum dots. Our goal is to determine the magnitude of the Knight field and the dipole-dipole field by monitoring the polarization of the photoluminescence (PL) under the influence of external magnetic fields of the order of millitesla. Furthermore, we use these results to estimate the maximum nuclear spin polarization and hence the nuclear field which can be achieved at zero external magnetic field.

II. SAMPLES AND EXPERIMENT

The sample studied is a 20 layer (In,Ga)As self assembled quantum dot ensemble with a dot density of 10^{10} cm^{-2} . 20 nm below each quantum dot layer a silicon δ -doping layer is located with a doping density about equal the dot density. Thus each quantum dot is permanently occupied with on average one “resident electron”, as confirmed by pump and probe Faraday rotation measurements [26]. The InAs quantum dot structure was grown by molecular beam epitaxy on a (100) GaAs substrate. After growth it has been thermally annealed for 30 seconds at 900°C. This leads to interdiffusion of Ga ions into the QDs, which shifts the ground state emission to 1.34 eV.

The measurements were performed at $T \leq 2$ K with the sample installed in an optical bath cryostat which was placed between three pairs of Helmholtz coils allowing application of external magnetic fields of a few mT in all directions. The coils were used to compensate parasitic magnetic fields, e. g. of geomagnetic origin as well as to apply fields up to 3 mT parallel or perpendicular to the optical axis (longitudinal, z direction or transverse, x direction, respectively).

The optical excitation was performed using a mode locked Ti:Sph pulsed laser with a pulse duration of 1.5 ps and a repetition rate of 75.6 MHz (pulses separated by 13.2 ns). The excitation energy was 1.459 eV which corresponds to the low energy flank of the wetting layer.

The helicity of the exciting light could be modulated by means of an electro-optical modulator and a $\lambda/4$ wave plate. Square pulses with either σ^+ or σ^- polarization and a rise time of a few nano seconds were generated. With this setup pulse trains with duration between 20 μs and 500 ms of σ^+ or σ^- polarization were formed.

The beam was focused on the sample with a 10 cm focus length lens which was simultaneously used to collect the PL. The photoluminescence was dispersed with a 0.5 m monochromator and detected circular polarization resolved with a silicon avalanche photo-diode which was read out using a two channel gated photon counter.

III. OPTICAL ORIENTATION OF ELECTRONS AND NEGATIVE CIRCULAR POLARIZATION

The studied quantum dots contain on average one “resident electron”. After excitation of an electron-hole pair

into the wetting layer and subsequent capture of the carriers into the quantum dot, a trion is formed. The trion ground state consists of two electrons with antiparallel spins and a hole. The helicity of the light emitted after the trion decays is therefore governed by the spin orientation of the hole.

It is an established phenomenon for n-doped quantum dots under nonresonant circularly polarized excitation and at zero magnetic field that the circular polarization ρ_c of the emission is negative with respect to the circular polarization of the excitation (negative circular polarization, NCP). This means that the intensity of the PL oppositely circularly polarized to the excitation polarization is greater than the intensity of PL having the same polarization as the excitation (using the standard definition: $\rho_c = (I^{++} - I^{+-})/(I^{++} + I^{+-})$, with I^{+-} denoting the intensity of PL having the same helicity as the excitation and I^{+-} denoting the intensity of PL polarized oppositely to the excitation). Figure 1 (a) depicts PL spectra of the studied QD ensemble under σ^+ excitation in the wetting layer, with detection either co-polarized (σ^+) or cross-polarized (σ^-) to the excitation. Both PL spectra show two peaks corresponding to the inhomogeneously broadened ground state emission at ≈ 1.34 eV (s-shell), and to the first excited state emission at ≈ 1.37 eV (p-shell). The polarization of the PL is negative for all emission from the s-shell (1 (a), upper panel).

Different mechanisms explaining the NCP effect were suggested [27, 28, 29, 30, 31, 32]. In all of them, however, the simultaneous spin flip of an electron and a hole spin (electron-hole spin flip-flop) is the key point. We examine the NCP effect with the view of determining the effect of NCP on resident electron polarization along the lines of [28]. In order to explain the effect of NCP, we assume that electron-hole pairs excited in the wetting layer, quickly relax into the dots conserving the spin of the electrons while the spin of the heavy hole is completely lost during relaxation. This is due to the fact that heavy-light hole mixing in the wetting layer and the excited quantum dot states destroys the hole polarization completely. This means that the hole itself retains no spin information from the excitation. The hole may rapidly relax to the ground state, the electron to the first excited state P_e and the resident electron shall occupy the lowest state in the conduction band.

With these assumptions, four different excited trion states are possible after circularly polarized excitation (Fig. 1(c): states with antiparallel electron spins and states where the electrons’ spins are parallel, each with the hole having either spin $+3/2$ or $-3/2$. Both sets of states should initially occur with the same probability.) Let us exemplarily consider the case of σ^+ excitation (photogenerated electron spin “down”, hole spin “up”, $\downarrow\uparrow$).

The configurations with antiparallel electron spins (Fig. 1 (c), ③ and ④) allow relaxation to the ground state. A ground state trion is formed: no spin information is contained in the antiparallel electrons, and the

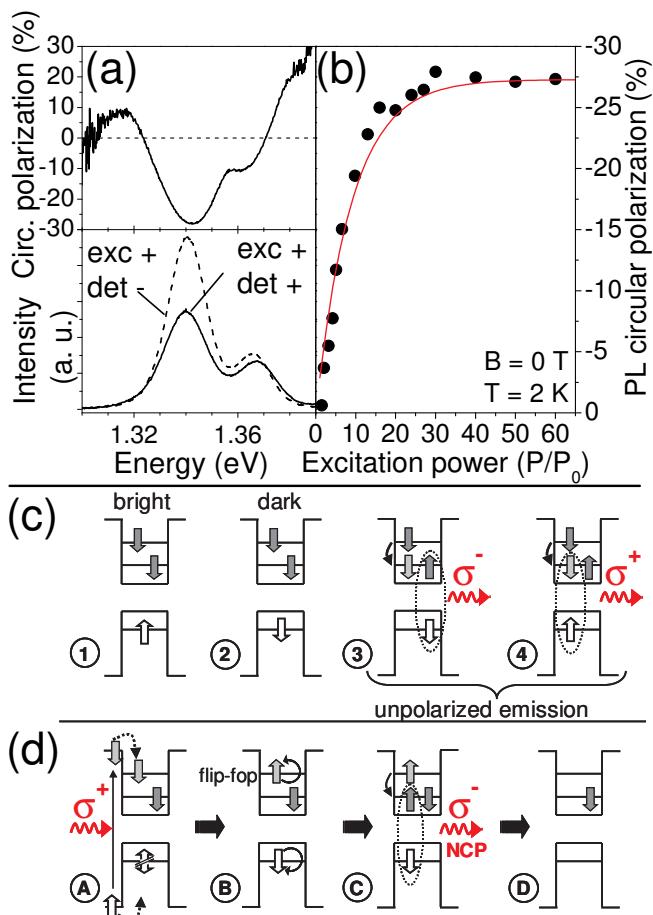


FIG. 1: (color online) (a) PL spectra of the studied QD sample (lower panel). Excitation was σ^+ at 1.459 eV. The PL intensity of σ^- emission is greater than that of σ^+ emission, thus the circular polarization of the PL is negative (upper panel). (b) Power dependence of the negative circular polarization (NCP) of the PL. The NCP rises with power and finally saturates indicating that a memory of the spin orientation of the resident electrons is kept until the following excitation cycle (see text). $P_0 = 2.5 \text{ W/cm}^2$. (c) The four possible hot trion configurations for σ^+ excitation assuming that the hole spin is lost during relaxation whereas the electron spin is kept. The singlet states 3 and 4 together yield unpolarized emission due to the random orientation of the hole. (d) NCP emission from the bright trion: The electron-hole spin flip-flop (B) is followed by relaxation to the groundstate (C). The ensuing radiative decay of the trion exhibits NCP. The resident electron is left behind polarized (D), maintaining its spin until the next excitation cycle (A) where the double arrow for the hole indicates that it loses its orientation during relaxation. The dark trion eventually also exhibits NCP (see text).

holes are also unpolarized. This trion state then decays producing unpolarized emission due to the random orientation of the holes.

The configurations with parallel electron spins are either bright (Fig. 1 (c), ①) or dark (Fig. 1 (c), ②). Relaxation of the electron in the p-shell to the s-shell will

not occur without a spin-flip due to Pauli blocking which dictates that the two electrons must have opposite spin. However, the anisotropic exchange interaction between electron and hole [33, 34] couples this state to the hot singlet trion (Fig. 1 (d), B): A synchronous reversal of the p-shell electron and the hole spin takes place (electron-hole spin flip-flop). This enables fast relaxation to the ground state. As the electron transfers spin to the hole, the hole is now polarized in the ground state trion configuration. Recombination therefore results in negative circular polarization (Fig. 1 (b), C).

For the dark trion this mechanism is by orders of magnitude weaker than for the bright trion because the flip-flop coupling term of the anisotropic exchange splitting is small for the dark electron-hole pairs. However, a single particle spin-flip of the electron due to the anisotropy of the quantum dot shape may occur, which allows transition to the trion ground state [27, 35]. In this case, the hole has undergone no spin flip, and the ground state again decays, emitting negatively polarized light. Some of the dark excitons may also undergo a nonradiative decay [28]. We observe therefore that both cases ① and ② result in NCP, whereas cases ③ and ④ result in unpolarized emission: the emission polarization is therefore predominantly negative.

The resident electron has a well-defined polarization after the decay of the trion (Fig. 1 (d), D). Its spin direction is the same as that of the hole and exactly determined by the polarization of the emitted photon. Measured over the ensemble, σ^+ excitation predominantly leads to σ^- emission and leaves behind a spin down electron polarization.

What is central to our experiment is that the resident electron partially retains its polarization until the next excitation cycle [27]. This leads to the accumulation of NCP over several excitation pulses. The quantum dots containing resident electrons which have already been polarized by the NCP effect again emit NCP with the following cycle, while in each cycle a fraction of the still unpolarized resident electrons become polarized [29, 36]. Figure 1 (b) shows the NCP value as a function of excitation power. The NCP increases with excitation power and eventually saturates. The degree of NCP is ultimately governed by the polarization retained by the photogenerated electron as it relaxes to the p-shell, the polarization of the resident electron and the ratio between radiative decay time of a hot bright trion and the spin flip-flop time. As the polarization memory of the photogenerated electron during relaxation and the flip-flop rate are unlikely to depend on the excitation power, the power dependence of the NCP should be due to the polarization memory of the resident electron which is likely to be a complicated function of the excitation conditions. Thus the power dependence of the NCP suggests that a memory of the excitation is kept by the resident electrons until the following excitation cycle [27].

In our studies we exploit these properties of the NCP effect: We use NCP both to create electron spin polar-

ization in our quantum dots and to *read out* the resident electron spin polarization ρ_e by monitoring the NCP amplitude of the photoluminescence. The projection of the average electron spin $\langle \mathbf{S} \rangle$ on the excitation axis (z direction), S_z , is related to the PL polarization ρ_c by

$$\rho_c \propto \frac{S_z}{S} \approx \rho_e, \quad (1)$$

and $S = 1/2$. ρ_c thus serves as a measure of the resident electrons' average S_z .

Note that there may also exist neutral quantum dots in the ensemble which might decay emitting slightly positively polarized light. This would lead to a constant offset in Eq. (1).

IV. ORIENTATION OF NUCLEI AND THE ELECTRON-NUCLEAR SPIN SYSTEM

As an electron inside a quantum dot is strongly localized, the interaction between electron spin and quantum dot nuclear spins is enhanced in comparison to bulk semiconductors. A single electron populating the ground-state of a quantum dot has a Bloch wavefunction with s -symmetry which has an overlap with about 10^5 quantum dot nuclei, estimated by considering an approximately disk shaped quantum dot 20 nm in diameter and 5 nm in height. Their spins interact with the electron spin via the hyperfine interaction. The hyperfine interaction is described by the Fermi contact Hamiltonian [37]

$$\hat{H}_{hf} = \sum_i A_i |\psi(\mathbf{R}_i)|^2 \hat{\mathbf{S}} \cdot \hat{\mathbf{I}}_i. \quad (2)$$

$|\psi(\mathbf{R}_i)|^2$ is the probability density of the electron at the location \mathbf{R}_i of the i^{th} nuclei, A_i is the hyperfine interaction constant and $\hat{\mathbf{S}}, \hat{\mathbf{I}}_i$ the spin operators of the electron spin and the nuclear spin respectively. Generally, the magnetic field generated by the sum of the nuclear spins is not zero, even in a randomly polarized system. The imbalance in the number of nuclei polarized in any particular direction is proportional to \sqrt{N} , where N gives the number of nuclei in contact with the electron. The result is an effective magnetic field B_f about which the electrons precess. B_f can be approximated by $B_f = B_{N,max}/\sqrt{N}$ with $B_{N,max}$ being the maximum nuclear magnetic field for 100% nuclear polarization. We estimate below a value of $B_{N,max} = 8.3$ T for our quantum dots. For $N \approx 10^5$ one thus obtains $B_f \approx 25$ mT. Experimental values of 10 to 30 mT for B_f agree well with this estimate [38]. This nuclear spin fluctuation (NSF) field changes on a timescale of 10^{-6} seconds [22]. As the precession of the electron in the hyperfine field of the nuclei is much faster than the dynamics of the nuclei in the field generated by the electron, the electron initially is exposed to a “snapshot” of B_f , where the nuclear spin configuration remains “frozen”. The direction and the magnitude of this frozen nuclear spin fluctuation, however, vary from dot to dot which leads to a rapid decay

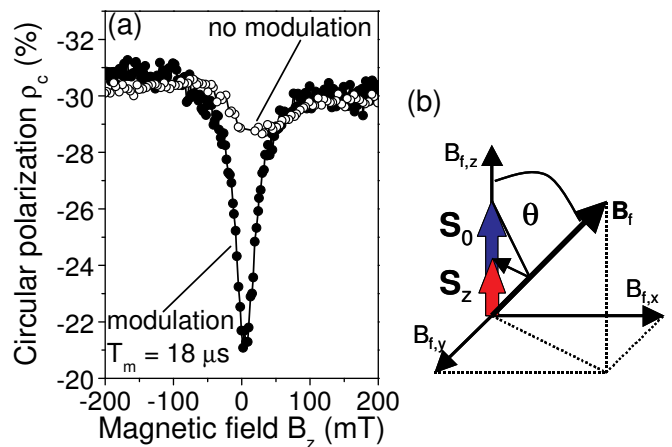


FIG. 2: (color online) (a) Dependence of the negative circular PL polarization on a longitudinal magnetic field. For fast modulation (full circles) no significant nuclear polarization can build up and at $B_z = 0$ the NSF lead to depolarization of the ensemble average S_z . When B_z becomes large enough to suppress the NSF field B_f the polarization is restored. Without modulation (open circles) nuclear polarization in z direction builds up and the influence of the transverse components $B_{f,x(y)}$ is reduced. This leads to a significantly higher electron polarization also at $B_z = 0$. Excitation density $P \approx 100$ W/cm². (b) The electron spin under the influence of the fluctuation field. \mathbf{S}_0 (blue arrow) precesses about the frozen fluctuation field \mathbf{B}_f , projection of \mathbf{S}_0 on the direction of \mathbf{B}_f reduces the z component of the electron spin to $S_z = S_0 \cos^2 \theta$ (red arrow).

of the average electron spin orientation in the ensemble (note that this is also true for single dots when the electron polarization is measured as an average over many excitation cycles).

The motion of a spin $\mathbf{S}(t)$ in a fixed magnetic field is described by

$$\begin{aligned} \mathbf{S}(t) = & (\mathbf{S}_0 \cdot \mathbf{b}) \mathbf{b} + (\mathbf{S}_0 - (\mathbf{S}_0 \cdot \mathbf{b}) \mathbf{b}) \cos \omega t + \\ & ((\mathbf{S}_0 - (\mathbf{S}_0 \cdot \mathbf{b}) \mathbf{b}) \times \mathbf{b}) \sin \omega t, \end{aligned} \quad (3)$$

where \mathbf{S}_0 is the initial electron spin, $\mathbf{b} = \mathbf{B}/B$ is the unit vector in direction of the magnetic field acting on the electron and ω is the Larmor precession frequency given by $\omega = |g_e| \mu_B B / \hbar$.

If we average the z component of $\mathbf{S}(t)$ over time we obtain

$$\begin{aligned} \bar{S}_z = & \frac{1}{\tau} \int_0^\infty S_z(t) \exp\left(-\frac{t}{\tau}\right) dt \\ = & \frac{S_0}{B^2} \left(B_z^2 + \frac{B_x^2 + B_y^2}{1 + \tau^2 \omega^2} \right), \end{aligned} \quad (4)$$

with B_j the $j = x, y, z$ component of the total field \mathbf{B} , and the lifetime τ of the electron spin, provided that \mathbf{S}_0 is parallel to the z axis with $S_{0,z} := S_0$. In the limit where the precession period $T \ll \tau$, $\tau^2 \omega^2 \rightarrow \infty$ and the expression for \bar{S}_z is obviously analogous to the projection

of the initial electron spin S_0 on the precession axis where the precession axis can be characterized by an angle θ to the z axis (see Fig. 2):

$$\begin{aligned}\bar{S}_z(\mathbf{B}) &= S_0 \frac{B_z^2}{B^2} \\ &= S_0 \cos^2(\theta(\mathbf{B})),\end{aligned}\quad (5)$$

$$\text{with } \theta(\mathbf{B}) = \frac{\pi}{2} - \arctan\left(\frac{B_z}{\sqrt{B_x^2 + B_y^2}}\right).\quad (6)$$

In the absence of an external magnetic field, only the internal field $\mathbf{B} = \mathbf{B}_f$ acts on the electron. Assuming that the nuclear spins are randomly distributed, $B_{f,x} = B_{f,y} = B_{f,z}$ and thus

$$\begin{aligned}\theta &= \frac{\pi}{2} - \arctan\frac{1}{\sqrt{2}} \triangleq 54.7^\circ \\ S_z &= \frac{S_0}{3}.\end{aligned}\quad (7)$$

For a randomly oriented nuclear spin system the electron spin polarization hence quickly decays to about 1/3 of its initial value due to the frozen NSF field. Total decay then follows on a microsecond timescale due to continuous change in direction of the NSF field [21, 22].

Strong optical pumping of the electron spins, however, may result in an orientation of the nuclear spins along the axis of excitation via spin flip-flops with polarized electrons (Overhauser effect). This transfer of angular momentum from the electrons to the nuclei is mediated by the hyperfine interaction. Continuous optical pumping realigns the electron after angular momentum transfer to a nucleus, such that many nuclei become oriented. While without optical orientation the nuclear fluctuation fields in every quantum dot of the ensemble are evenly distributed in all three dimensions, optical orientation leads to a decrease of the inplane components $B_{f,x}$ and $B_{f,y}$ in favour of the z component $B_{f,z}$:

$$B_{f,z} > B_{f,x(y)}.\quad (8)$$

The electrons now precess about a nuclear field whose z component dominates, resulting in an increase of average electron spin polarization S_z in comparison to the case of a totally randomly oriented nuclear system. The angle θ in Eq. (6) decreases and S_z increases.

A significant nuclear polarization obtained by strong pumping and sufficiently long illumination of the sample leads to a nuclear field $B_N \gg B_{f,x/y}$ parallel to z and a marked reduction of the influence of the NSF, maximally restoring electron spin alignment in z direction [38].

Fig. 2 (a) illustrates the effect of nuclear polarization. Two curves are shown displaying the dependence of the PL polarization on an external field in z direction, one of them obtained for modulation between σ^+ and σ^- excitation with period $T = 18 \mu s$ (with measurements performed during the σ^+ cycle only), the other one for

unmodulated excitation, i. e. constant σ^+ excitation. Let us first consider the external field dependence of the PL polarization for modulated excitation, where no significant nuclear field B_N builds up (we will demonstrate in Sec. V.A that significant nuclear polarization requires tens of milliseconds pumping time). In this case, the NSF reduce the electron polarization at $B_z = 0$ to about 21 %. When B_z is increased, the resultant field $\mathbf{B} = \mathbf{B}_{ext} + \mathbf{B}_f$ is at an angle closer to the z axis ($\theta' < \theta$). The projection of the electron polarization, given by Eq. (5), increases from ≈ 21 % to ≈ 30 %. For values $B_{ext} \gg B_f$, $\theta' \approx 0$ and the PL polarization saturates at ≈ 31 %.

We now compare this to the case where a nuclear field is allowed to accumulate. Unmodulated excitation causes optical orientation of the nuclear spins even at $B_z = 0$ and a nuclear field B_N in z direction builds up. This nuclear field plays exactly the same role as an external field in increasing the projection of the electron spin onto the z axis. The resultant field onto the electron, given by $\mathbf{B}_f + \mathbf{B}_N$, is, again, closer to the z axis. In this case, B_N dominates over B_f . The polarization reaches ≈ 29 % already at $B_z = 0$, demonstrating that for almost all quantum dots, a significant nuclear polarization must occur.

The process of orienting the nuclear spins via optically pumped electrons, however, is slow and maximum polarization of the nuclear system can take as long as tens of milliseconds [18, 25]. The fastest depolarizing mechanism of the nuclear spins is the dipole-dipole interaction between a nuclear spin and its neighbouring nuclei, the magnitude of which may be represented by a magnetic field, the dipole-dipole field B_L . It acts on a timescale of 10^{-4} seconds generally impeding the build up of nuclear polarization. Nevertheless, nuclear polarization can build up if the dipole-dipole field is overcome by a magnetic field greater than the magnitude of B_L or, surprisingly, when a magnetic field with magnitude comparable to B_L is present. In the latter case, an effective energy exchange between the Zeeman part and the dipole-dipole part of the nuclear energy can occur leading to a lowering of the nuclear spin temperature by the interaction with spin oriented electrons [7, 39].

Such a small magnetic field in z direction is provided by the z component of the resident electron spin. This field, the Knight field B_e , is antiparallel to the electron spin and its direction is thus determined by the exciting photon's helicity. It is proportional to the average spin of the resident electron [7, 8]:

$$\mathbf{B}_e = b_e \frac{\langle \mathbf{S} \rangle}{S} = 2b_e \langle \mathbf{S} \rangle$$

where b_e gives the average Knight field for a fully polarized electron at a particular nuclear site [7, 8]. The Knight field thus may enable nuclear polarization to occur in the absence of an external longitudinal field.

In fact it was shown that nuclear polarization can be achieved for quantum dots in zero magnetic field [15, 19].

In our measurements, the fact that we observe a reduction of the influence of the NSF even at vanishing external fields indicates that we also accumulate nuclear polarization in our quantum dots at zero field (Fig. 2, see also [25, 38]). Further proof of zero field nuclear spin polarization in our sample is discussed in connection with the Hanle measurements in the following section.

The nuclear field in the presence of an electron spin S is generally calculated via the nuclear polarization which is given by the equation [5, 7, 37]

$$\frac{\langle \mathbf{I} \rangle}{I} = B_I(x(S)), \quad (9)$$

where B_I is the Brillouin function for a particular nuclear spin I ,

$$B_I(x(S)) = \frac{2I+1}{2I} \coth\left(\frac{2I+1}{2I}x\right) - \frac{1}{2I} \coth\left(\frac{1}{2I}x\right), \quad (10)$$

and

$$x(S) \approx I \ln\left(\frac{1+2S}{1-2S}\right) \quad (11)$$

under the condition of optical orientation. For small values of S and I , it is a good approximation to only consider the first term of the expansion of the Brillouin function in S ,

$$B_I^{(1)} = \frac{4}{3}(I+1)S. \quad (12)$$

The vector generalization of Eq. (12) to the case of small external magnetic fields is then given by ([7], chapter 2,[39])

$$\frac{\langle \mathbf{I} \rangle}{I} = \frac{4}{3}(I+1) \frac{(\langle \mathbf{S} \rangle \cdot \mathbf{B}) \mathbf{B}}{B^2 + B_L^2}. \quad (13)$$

\mathbf{B} is the sum of the internal Knight field and an external field, $\mathbf{B} = \mathbf{B}_{ext} + b_e \langle \mathbf{S} \rangle$, and $\langle \mathbf{S} \rangle$ is the average resident electron spin. With the relation

$$\begin{aligned} \mathbf{B}_N(\mathbf{B}_{ext}) &= \sum_i b_{N,i} f_i \frac{\langle \mathbf{I}_i \rangle}{I_i} \\ &= \frac{4}{3} f b_N' \frac{(\langle \mathbf{S} \rangle \cdot \mathbf{B}_{ext} + 2b_e \langle \mathbf{S} \rangle^2)}{(\mathbf{B}_{ext} + 2b_e \langle \mathbf{S} \rangle)^2 + B_L^2} (\mathbf{B}_{ext} + 2b_e \langle \mathbf{S} \rangle) \end{aligned} \quad (14)$$

we can calculate the nuclear field $\mathbf{B}_N(\mathbf{B}_{ext})$. i denotes the particular nuclear species, indium, gallium and arsenic in our case, $b_{N,i}$ is the field of the i^{th} nuclear species for the case of 100 % nuclear polarization and $b_N' = \sum_i b_{N,i}(I_i + 1)$. The leakage factor f accounts

for losses of nuclear spin polarization. For $\text{In}_{0.5}\text{Ga}_{0.5}\text{As}$ quantum dots it was estimated that [8, 23, 40]

$$\begin{aligned} b_{N,\text{In}_{50\%}} &\approx -4.3 T \\ b_{N,\text{Ga}_{50\%}} &\approx -1.26 T \\ b_{N,\text{As}} &\approx -2.76 T. \end{aligned} \quad (15)$$

With these values we obtain a maximum nuclear field of $B_{N,max} = \sum_i b_{N,i} = -8.3 T$.

Note though that the approximation of linearizing the Brillouin function is only good if the electron polarization $\langle \mathbf{S} \rangle$ is small [5, 8]. The error becomes greater the bigger the nuclear spin I is. For indium with $I = 9/2$, a deviation of $\approx 10\%$ between $B_I(x)$ and $B_I^{(1)}(x)$ is already reached for $\langle S \rangle \approx 0.06$.

In order to estimate the ability of the electron-nuclear system to become polarized under optical orientation it is necessary to determine the magnitude of the Knight field B_e and the dipole-dipole field B_L . We will show in the following sections that the behavior of the nuclear field is strongly influenced by millitesla external magnetic fields. The dependence of the PL polarization on the magnitude and the direction of such small fields can be exploited to determine the important quantities B_L and B_e .

V. RESULTS AND DISCUSSION

A. Hanle type measurements and the dipole-dipole field

When spin oriented electrons are exposed to a magnetic field perpendicular to their spin orientation they start to precess about this field, as described in Eq. (3). For a single electron spin, the projection onto the z axis will oscillate sinusoidally with time, until the electron spin is either re-initialized or it loses its phase information (spin coherence). Therefore, in a perpendicular magnetic field the value of S_z is governed by competition between the precession frequency of the electron spin and the time at which the spins are either re-initialized or decohere. The projection of their spin on the z axis, S_z , decreases the further they precess. If the precession is terminated by the radiative decay of the electron (in the case of neutral QDs), re-initialization of its spin (in our case of negatively charged QDs) or by spin relaxation, the spin polarization measured will be the value of S_z at that point. As the precession frequency is proportional to the magnitude of the field the electron spin precesses further the higher the field and thus loses increasingly more of its z component. Monitoring S_z via the PL polarization on sweeping the transverse field yields a Lorentzian curve the width of which is inversely proportional to the spin life time of the electron T_2^* where $1/T_2^* = 1/\tau_r + 1/\tau_s$, τ_r is the electron reinitialization time and τ_s the spin relaxation time:

$$T_2^* = \frac{2\hbar}{|g_{e,x}| \mu_0 B_{1/2}}, \quad (16)$$

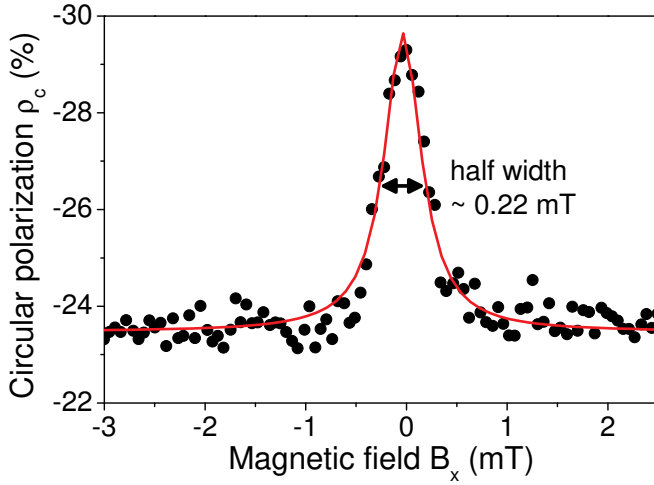


FIG. 3: (color online) Dependence of the PL polarization on a transverse magnetic field B_x under continuous circularly polarized excitation (full circles: measured data, solid line: Lorentz fit). When the external field is strong enough to overcome B_L the nuclear field realigns towards the x axis and the electron spins become depolarized by precession about the x component of the nuclear field. For $B_x > B_L$ the electrons become completely depolarized, no nuclear polarization is generated anymore and the electron spin is left with the NSF field. Excitation density $P \approx 100 \text{ W/cm}^2$.

with the electron g factor $g_{e,x}$ along x , and the half width $B_{1/2}$ of the Lorentz curve. This is known as Hanle effect (W. Hanle 1924, [41], and e. g. [42]).

Fig. 3 shows a graph obtained from a Hanle type measurement under continuous excitation on our quantum dot sample. A transverse magnetic field B_x was swept and the PL polarization for each field value was recorded. The PL polarization drops sharply from its maximum value at $B_x = 0$ the half width of the peak being $\approx 0.2 \text{ mT}$. From equation (15), this would correspond to a value of $T_2^* 114 \text{ ns}$.

Let us now consider what happens if the excitation helicity is flipped between σ^+ and σ^- with period T_m that we are able to vary over a range of milliseconds. Fig. 4 (a) shows Hanle curves under excitation modulated in such way. The narrow peak appearing with unmodulated excitation becomes broader and gradually disappears when the modulation frequency is increased. It almost completely vanishes for a modulation period of $T_m = 1 \text{ ms}$. This value is in complete disagreement with the value obtained from Equation 15. Moreover, as the dynamics of the electron takes place on a nanosecond timescale, this millisecond effect is far too long to be of electronic origin. Although transverse fields also lead to the depolarization of polarized electron spins in the quantum dots under study, the situation obviously fundamentally differs from the one underlying the original Hanle effect.

The strong influence of the excitation modulation on the peak in our Hanle type measurements arises due to the influence of the quantum dot nuclei which need tens

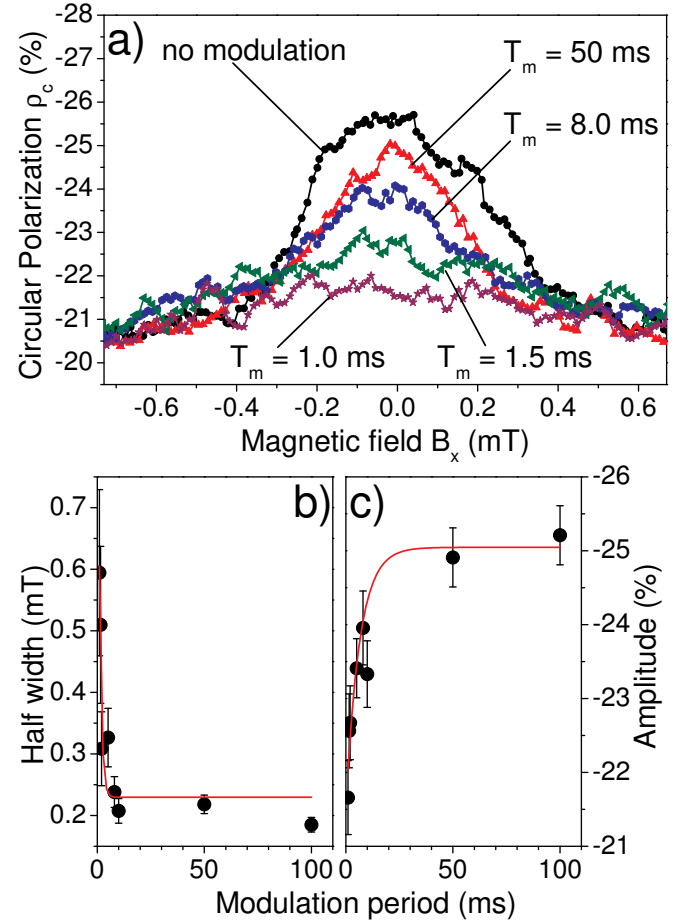


FIG. 4: (color online) (a) Hanle curves for excitation modulated between σ^+ and σ^- with period T_m (smoothed). The narrow peak gradually vanishes the faster the modulation becomes and almost is absent for $T_m = 1 \text{ ms}$ because nuclear polarization is more and more obstructed the faster the modulation is. Excitation density $P \approx 50 \text{ W/cm}^2$. (b) Half width at half maximum of the Hanle peaks for different modulation periods T_m . Red line: Exponential decay fit. (c) Absolute peak amplitude for different modulation periods T_m . The faster the modulation the smaller the nuclear field and the bigger the influence of the random fluctuation field. Red line: Asymptotic fit.

of milliseconds to become polarized [18]. The resident electron is generally influenced by the nuclear field whose magnitude and direction are highly dependent on the external field [7, 8]. Particularly, in the range of weak external fields, this results in a behavior of the electron spin that is predominantly governed by the nuclear field. Thus, care has to be taken when the width of the Hanle peak is used to determine the spin lifetime of the electron in quantum dots as has been suggested in the literature [42, 43, 44]. At fields lower than several tens millitesla the nuclear field or the frozen fluctuation field will always dominate the spin dynamics.

In the following we will explain the mechanisms leading to the specific shape of the Hanle curve. In particular,

we focus on the two main features of the curve: (i) the width of the Hanle peak and (ii) the surprising fact that the polarization at first remains on a relatively high level outside the peak even though the transverse magnetic field is increased further.

For unmodulated excitation nuclear spin polarization and with it a nuclear magnetic field builds up along the z axis when $B_x = 0$. The nuclear field adds to the frozen fluctuation field B_f and reduces the angle θ between the z axis and the total nuclear magnetic field $B_{N,tot} = B_N + B_f$ which supports electron spin polarization as discussed in Sec. IV. Thus a significant nuclear field has been shown to build up. When a transverse field B_x is switched on, each nucleus now experiences a field from the electron, $2b_e\langle\mathbf{S}\rangle$, and the external field \mathbf{B} . The nucleus realigns itself to the sum total field $\mathbf{B} + 2b_e\langle\mathbf{S}\rangle$, and the macroscopic nuclear field B_N aligns along this direction.

The electron spin only precesses about $B_{N,x} \parallel B_x$. The nuclear field component parallel to the Knight field does not influence the precession as $2b_e\langle\mathbf{S}\rangle \parallel \mathbf{B}_e \parallel \mathbf{S}$. Under the influence of an external field in x direction the electron spin thus experiences a purely transverse field, the external field amplified by the x component of the nuclear field. Consequently, the electron spin precesses in the z - y -plane.

Thus the field B_N is aligned along $\mathbf{B} + 2b_e\langle\mathbf{S}\rangle$, i.e. the sum of the external and Knight fields. The Knight field, however, is not constant: it decreases in as much the electron spin becomes depolarised by precessing about the strong transverse nuclear field. A transverse field of strong magnitude would lead to a complete depolarization of the electron spin before it becomes reinitialized with the next excitation event.

We observe though that the polarization does not immediately drop to zero when a transverse field is present. The depolarization peak is in fact about 0.4 mT wide. This fact may be explained by the presence of the dipole-dipole field B_L . For external magnetic fields $B_x < B_L$ the external field is screened by B_L . In order to realign the nuclear spins, B_x has to dominate over the dipole-dipole field. As for measurements in a purely transverse magnetic field the x component of the Knight field is zero, the only transverse field experienced by the nuclear spins is the external field. The width of the Hanle peak is hence solely determined by the competition between B_L and B . This is discussed further in [7].

We shall now examine what happens when B_x is increased above the magnitude of B_L and why the polarization remains at a constant level for $B_x \gtrsim 0.6$ mT, and does not drop to zero, as may be expected if the field B_N is purely transverse. To understand this behaviour, one must consider the magnitude of the nuclear polarization field B_N relative to the fluctuation field B_f . The field B_N will decrease as B_x increases: this is due to the fact that B_N is dependent on $\langle\mathbf{S}\rangle$ and decreases with decreasing electron spin. Thus, at a significantly large B_x , $B_N < B_f$. The fluctuation field then dominates the

electron spin dynamics, and the NCP value reaches $\approx 23\%$, the value found at 0 T in Fig 2 (a) for modulated excitation (i.e. with no nuclear polarization).

Let us come back to Fig. 4. Figure 4 (c) shows the amplitude of the depolarization peak in dependence of the modulation period T_m . As the time to maximally polarize the nuclear spins lies in the millisecond range, modulating the excitation between σ^+ and σ^- limits the nuclear polarization in the direction specific to the particular excitation helicity that can be achieved in each excitation cycle. The PL amplitude saturates at $T_m \approx 40$ ms which allows us to estimate that the nuclear spins need ≈ 20 ms in order to become maximally polarized. Note that the time to polarize the nuclei also depends on the excitation density. We measure, however, always in the power regime where the NCP saturates (see Fig. 1 (b)).

Figure 4 (b) depicts the dependence of the half width of the peak for different modulation periods T_m . For $T_m < 10$ ms the peak is broadened by the fact that the nuclear field is only little larger than the frozen fluctuation field. The total Overhauser field is given by $B_{tot} = B_N + B_f$: even if the angle of B_N to the z axis makes changes from 0° to 90° , the variation in angle of B_{tot} is less. This means the depolarizing effect of the nuclear field is smeared out, and the curve becomes broader. The half width becomes saturated for $T_m \geq 50$ ms at about 0.22 mT for nuclear fields significantly outranging B_f . In this regime the width of the depolarization peak is a measure for the dipole-dipole field B_L as discussed above. The average peak half width from several measurements corresponds to a dipole-dipole field of

$$B_L = 0.22 \pm 0.02 \text{ mT.} \quad (17)$$

B. The Knight field

As discussed in Sec. IV, a magnetic field, the Knight field, is associated with the spin of the resident electron. The Knight field plays a significant role in the behavior of the electron-nuclear spin system in quantum dots: It provides a magnetic field in z direction which enables nuclear polarization to build up without the help of an external field along the optical axis. The Knight field is parallel to the electron spin and its z component is thus parallel or antiparallel to the excitation axis – depending on the excitation helicity. In order to determine the magnitude of the Knight field's z component we therefore measure the dependence of the PL polarization on a magnetic field along the z direction: If a magnetic field B_z parallel to the exciting laser is applied, there should eventually be a point where the external magnetic field is equal in magnitude but antiparallel to the Knight field.

Figure 5 depicts the B_z dependence of the polarization. The PL polarization exhibits a barely discernible dip which is offset from $B_z = 0$. The shift corresponds to the external field which is necessary to compensate the Knight field. In this compensation point the effective field $B_{eff} = B_z + B_e$ on the nuclei is minimised,

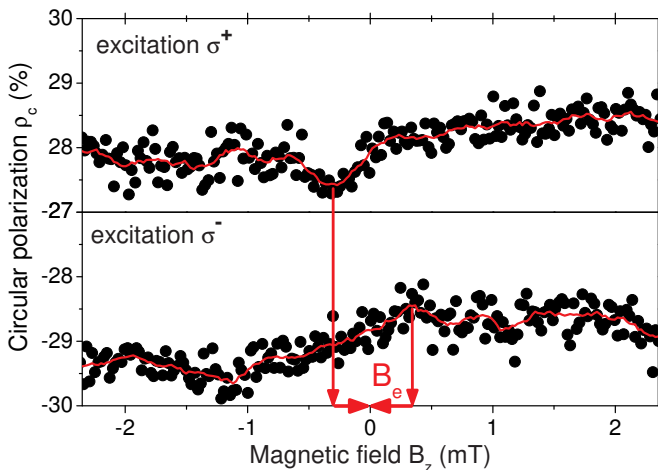


FIG. 5: (color online) B_z dependence of the PL polarization (NCP) for $B_x = 0$ and continuous excitation (full circles: measured data, solid line: smoothed). The dip at $B_{eff} = 0$ is shifted from $B_z = 0$ by the value of the Knight field B_e . Excitation density $P \approx 100$ W/cm².

such that $B_z = -B_e$. Examination of Eq. (14) demonstrates that at this point the nuclear polarization should drop to zero. The only field felt by each nucleus is the dipole-dipole field B_L , which causes depolarization on a scale 10^{-4} s, and no polarization should occur. Dynamic nuclear polarization is hindered and the only field on the electron in this point is the frozen random fluctuation field B_f leading to a reduction of the electron spin polarization.

However, the effect is very small when scanning the z -field. We will show in the next section that the nuclear fields may reach an average of ≈ 4 T, a value far greater than the fluctuation field B_f . Thus, compensation of the Knight field must be very accurate if the value of B_N is to be decreased by the three orders of magnitude needed to observe a drop in polarization. The compensation of the Knight field, however, cannot be perfect as the Knight field is inhomogeneous over the quantum dot. Additionally, the situation varies from dot to dot in the ensemble. Consequently, some nuclear polarization may still occur in the compensation point.

In order to enhance the effect, we additionally apply a constant transverse magnetic field B_x , and again step the B_z field. This technique, also used extensively in [8], allows one to access nuclear polarization regimes where B_N is smaller, without significantly changing the electron spin polarization generated (as it is for example the case by decreasing the power). In this technique, a transverse field is applied of magnitude 1.13 - 2.27 mT. As we have already observed in Section A, these B_x field values do not allow significant nuclear polarization to arise. The z -field is then swept, and the polarization measured. By keeping the B_x field constant and sweeping B_z , one effectively sweeps the angle that the total field $B_{tot} = B_x + B_z$ makes with the z -axis.

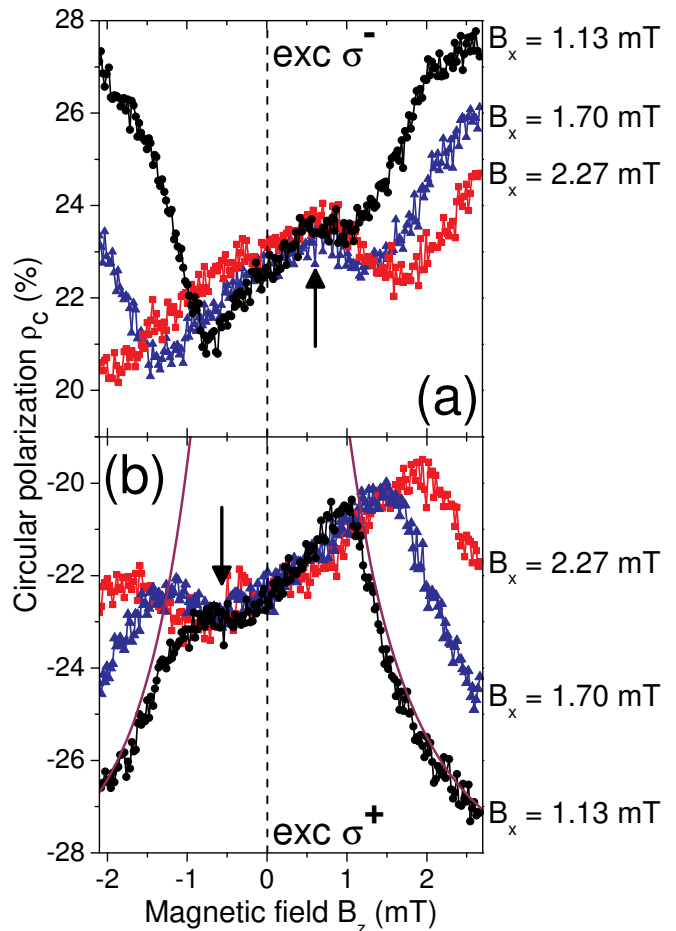


FIG. 6: (color online) B_z dependence of the PL polarization for different values of B_x : 1.13 mT, 1.7 mT and 2.27 mT. Excitation σ^+ (b) and σ^- (a). The constant shift of the peak in the middle of the W-shaped structure (indicated by arrows) corresponds to the magnitude of the Knight field. Solid line in (b): Polarization behaviour expected when the Knight field and the fluctuation field are neglected. Dashed line: $B_z = 0$. Excitation density $P \approx 100$ W/cm².

The solid line in Fig 6 (b) shows the polarization behaviour expected when the Knight field and the fluctuation field are neglected, and we consider that B_N is parallel to B_{tot} . The B_N field direction would vary from $\theta = 90^\circ$ at $B_z = 0$ T to $\theta = 0^\circ$ at $B_z \gg B_x$, and the time averaged electron spin $\langle \mathbf{S} \rangle$ would follow it also.

In Fig. 6, B_z dependences for various applied transverse fields are shown. The PL polarization exhibits a pronounced W-shaped behavior on sweeping the longitudinal field, that is inverted on changing the excitation helicity. Let us consider first the points indicated by arrows in Fig. 6, corresponding to local maxima in the curve. We note that at these points, the NCP reaches a value of ≈ 23 % for all values of B_x , and moreover, that these points, approximately correspond in magnitude and sign to the Knight field values observed in Fig. 5. At this point, the B_z field compensates the Knight field for many

of the QD nuclei. Any small nuclear field B_N that would be allowed to built up in the geometry defined by the external fields is suppressed, due to cancellation of the Knight field. Thus the NCP value measured corresponds to the fluctuation field value of $\approx 23\%$.

The marked asymmetry in the curves that are inverted when changing helicity allow easy determination of the compensation point. As soon as the B_z field is swept away from the compensation point, nuclear polarization may begin to occur, whose magnitude and direction appear to follow a complicated, non-linear behaviour. A full explanation of the complex behaviour of the curves is beyond the scope of this paper: however, we will phenomenologically examine some of the features observed.

Let us consider the behaviour at values of $B_z = B_e$, such that the total field on the nuclei is approximately equal to ≈ 1 mT. For all values of B_x measured, the NCP value is actually smaller than at the compensation point. This occurs due to the fact that a small nuclear polarization may occur. However, when this nuclear polarization is generated, it will be aligned along B_{tot} , which has a much greater angle to the z axis than the B_f angle of 54° . However, not much nuclear polarization can be generated due to the presence of the transverse field. The nuclear field thus is small and does not depolarize the electron too much. Any nuclear polarization generated will lead to a drop in NCP, until the B_z field becomes greater than B_x . At this point the NCP will increase again. We note that behaviour at these turning points is clearly dependent on the Knight field orientation: the curve is highly asymmetric. It is therefore clear that the Knight field has a significant effect on the electron-nuclear dynamics even when the applied field is much larger than the Knight field.

It is also apparent that, on sweeping the B_z field away from the compensation point, the NCP always decreases at first with B_z , even though one would expect that increasing B_z would lead to an increase in $\langle S \rangle$. However, it appears that the magnitude of nuclear polarization achieved is strongly dependent on the magnitude and direction of the external field. Upon applying a slightly larger B_z field, more nuclear polarization is achieved, which for values of $B_x > B_z$ leads to a decrease in NCP.

In order to evaluate the Knight field we determine in Fig. 6 the magnetic field at which the Knight field was compensated. This compensation point has an average position of

$$|B_e| = 0.5 \pm 0.1 \text{ mT}. \quad (18)$$

This agrees well with the value of 0.6 mT which was measured in single QD dot experiments [19].

C. Calculation of the nuclear field

The information we have gained about the magnitude of the Knight field and the dipole-dipole field enable us to estimate the magnitude of the nuclear magnetic field,

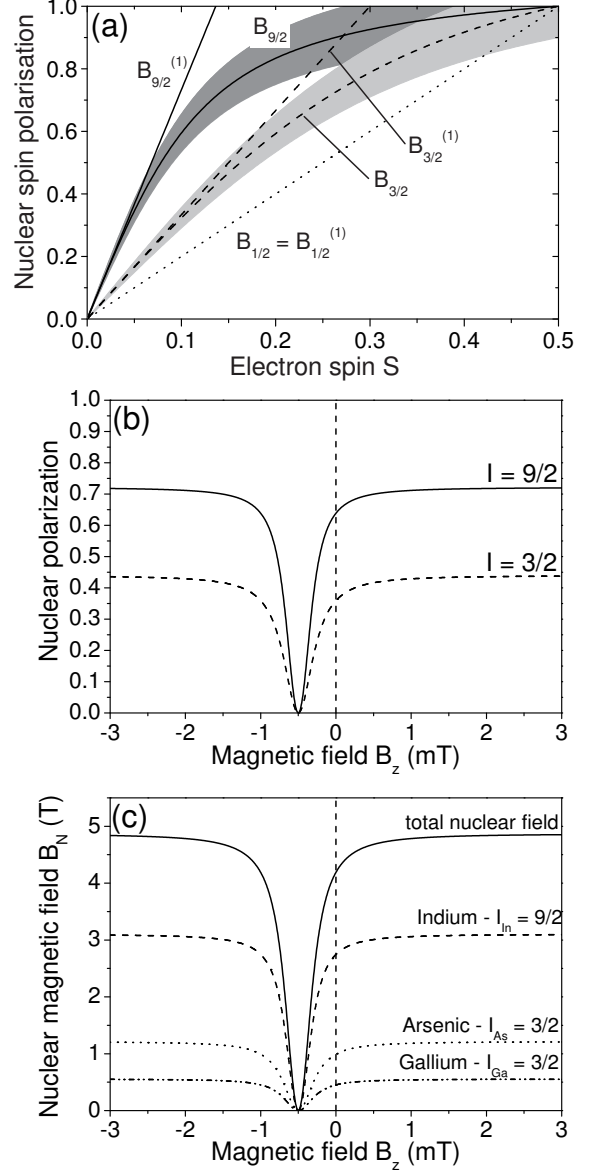


FIG. 7: (a) Comparison between the Brillouin functions for $I = 9/2$ (indium), $B_{9/2}(x)$ (solid line), $I = 3/2$ (gallium, arsenic), $B_{3/2}(x)$ (dashed line), and the first term of their expansions in S , $B_{9/2}^{(1)}$ and $B_{3/2}^{(1)}$. The shaded area illustrates the region of 10% deviation from $B_{9/2}(x)$ ($B_{3/2}(x)$). Above $S \approx 0.06$ the linearization is no longer a good approximation for indium. For $I = 1/2$, $B_{1/2} = B_{1/2}^{(1)}$. (b) The nuclear polarization under optical orientation for $I = 3/2$ nuclei (dashed line) and $I = 9/2$ nuclei (solid line) in dependence on a longitudinal external field B_z , calculated with Eq. (26). $\langle S_z \rangle = 0.145$. Without losses, the indium nuclei reach a polarization of $\approx 72\%$. (c) The nuclear field for the three different nuclear species (dashed line: indium, dotted line: arsenic, dash-dotted line: gallium) and the sum of the three, the average total nuclear field (solid line), calculated with Eq. (27). $B_{N,tot}$ becomes as large as ≈ 4.9 T. At $B_z = 0$, $B_{N,tot} \approx 4.2$ T.

$\mathbf{B}_N(\mathbf{B}_{ext})$. In the calculations the leakage factor f was set to one so that the results should be understood as the maximum polarisation which could be generated with the measured values $B_e = 0.5$ mT and $B_L = 0.22$ mT. As we have already mentioned in Sec. IV, Eq. (13), which was obtained by only retaining the linear term of the expansion of the Brillouin function, is not a good approximation anymore for Indium ($I = 9/2$) and $S > 0.06$ (see Fig. 7). In order to calculate the nuclear field under the influence of a small longitudinal external field for the (In,Ga)As quantum dots under study, we therefore cannot use this approximation. Instead of taking only the linear term of the power series of $B_I(x(S))$ into account (see Eqs. (12,13)) we therefore obtain the vector generalization of $\langle I \rangle$ by performing the substitution

$$S \longrightarrow \mathbf{S}_B = \frac{\langle \mathbf{S} \rangle \cdot (\mathbf{B}_{ext} + 2b_e \langle \mathbf{S} \rangle)}{(\mathbf{B}_{ext} + 2b_e \langle \mathbf{S} \rangle)^2 + B_L^2} (\mathbf{B}_{ext} + 2b_e \langle \mathbf{S} \rangle) \quad (19)$$

in all orders of the expansion which only contains odd powers of S . This leads to the formal expression

$$\langle \mathbf{I} \rangle = I \sum_{n=0}^{\infty} \frac{1}{n!} \left. \frac{d^n B_I(x(S))}{dS^n} \right|_{S=0} (\mathbf{S}_B)^n \quad (20)$$

$$= I \sum_{n=0}^{\infty} \left(\frac{1}{n!} \left. \frac{d^n B_I(x(S))}{dS^n} \right|_{S=0} S_B^n \right) \frac{\mathbf{S}_B}{S_B} \quad (21)$$

$$= I B_I(x(S_B)) \frac{\mathbf{S}_B}{S_B}, \quad (22)$$

with \mathbf{S}_B defined by Eq. 19. Under the conditions of optical orientation and codependent electron and nuclear spin polarizations it can be shown that [7, 8]:

$$\langle \mathbf{S} \rangle \cdot \langle \mathbf{S} \rangle = \langle \mathbf{S} \rangle \cdot \langle \mathbf{S}_0 \rangle, \quad (23)$$

$$\langle \mathbf{S} \rangle \cdot \mathbf{B}_{ext} = \langle \mathbf{S}_0 \rangle \cdot \mathbf{B}_{ext}. \quad (24)$$

With these relations we obtain

$$\mathbf{S}_B = \frac{\langle S_0 \rangle B_z + 2b_e \langle S_0 \rangle \langle S_z \rangle}{B_{ext}^2 + 4b_e \langle S_0 \rangle B_z + 2b_e^2 \langle S_0 \rangle \langle S_z \rangle + B_L^2} (\mathbf{B}_{ext} + 2b_e \langle \mathbf{S} \rangle) \quad (25)$$

where B_z is the longitudinal external field. For a system under the influence of a purely longitudinal external magnetic field electron as well as nuclear spins become exclusively polarized along the z axis. In this case we substitute $S_{B,z}$ for S in the argument of the Brillouin function, Eq. (22). We thus obtain for the nuclear polarization of a nuclear species with spin I

$$\frac{\langle I_z \rangle}{I} = B_I(x(S_{B,z}))$$

with $S_{B,z} = \frac{(B_z + 2b_e \langle S_z \rangle)^2}{(B_z + 2b_e \langle S_z \rangle)^2 + B_L^2} \langle S_0 \rangle$. (26)

The nuclear magnetic field is then given by

$$B_{N,z}(B_z) = \sum_i b_{N,i} f_i B_I(x(S_{B,z})) \quad (27)$$

where f is a leakage factor which accounts for any other phenomenological losses of nuclear polarization. From Fig. 6 we extract the average resident electron spin $\langle S_0 \rangle = \langle S_z \rangle = \rho_c/2 \approx -0.29/2$.

Figure 7 shows the nuclear polarization calculated with Eq. (26) and the nuclear fields calculated with Eq. (27) in dependence on a millitesla external field along the z axis. Neglecting losses, the nuclear polarization of indium saturates at $\rho_{In} \approx 72$ % and for gallium and arsenic at $\rho_{Ga/As} \approx 44$ %. With these values and $b_{N,i}$ from Eqs. (15), we calculate a maximum total nuclear field $B_N \approx 4.9$ T. At zero external field the nuclear field is already $B_N(0) \approx 4.2$ T.

These values are, however, only ensemble averages as they were calculated using the average electron polarization measured over the whole ensemble. There might be a significant fraction of quantum dots in the ensemble containing a resident electron which has a polarization close to unity whereas some quantum dots may contain unpolarized resident electrons. For instance, in our previous work [23], the formation of an ultra-stable "polaron" state was observed, where the electron polarization is close to unity. Full electron spin preservation is predicted in this case: this means that the magnitude of the Knight field reaches its maximum value, $b_e = B_e/(2\langle S \rangle)$, corresponding to $b_e \approx 1.7$ mT for $\langle S \rangle/S = 0.29$. In quantum dots where the resident electron polarization is $\rho_e \approx 1$ the indium polarization at zero external field is already as large as $\rho_{In} \approx 97$ % and the gallium and arsenic polarizations $\rho_{In} \approx 92$ %. This leads to a total nuclear field at zero applied external field of 7.9 T. Even if the losses were high, a considerable nuclear field of the order of Tesla should be present in many of the quantum dots.

VI. SUMMARY AND CONCLUSIONS

We have demonstrated that the effect of negative circular polarization may be used both to polarize the spins of the resident electrons in n-doped quantum dots and to optically orient the nuclear spins in the quantum dots via constant spin transfer from the spin oriented electrons. Furthermore, the spin polarization of the resident electrons may be read out by measuring the circular polarization of the photoluminescence upon circularly polarized excitation of the quantum dots.

The electron spin polarization at the same time serves as a sensitive detector for the state of the nuclear spin system. Millitesla external magnetic fields may be used to manipulate the nuclear spins which in turn amplify the external field by orders of magnitude making it possible to detect their action via the electron polarization. Exploiting this codependence of electron and nuclear spins, by studying Hanle curves for excitation modulated between σ^+ and σ^- helicity with different modulation periods we were able to show that it takes tens of milliseconds to maximally polarize the nuclear spin system in the quantum dots. It became obvious that one has to

examine thoroughly if Hanle measurements in a specific case can be used to determine spin relaxation times of the electron. Even when nuclear polarization is suppressed by modulated excitation the random nuclear field is still present possibly dominating the dynamics of the electron spins. Thus one may conclude that determining the electron spin lifetime using the Hanle effect for magnetic fields less than a few tens of millitesla is incorrect due to screening either from the fluctuation field or the dynamic polarization: an alternative method must be used.

The Hanle measurements also allowed us to determine the dipole-dipole field $B_L \approx 0.22$ mT. Furthermore, the magnetic field dependence of the PL polarization in a combination of Faraday and Voigt geometries could be used to obtain an accurate determination of the magnitude of the Knight field $B_e \approx 0.5$ mT.

After having determined the important quantities of the electron-nuclear spin system the nuclear field under the influence of a longitudinal external magnetic field could be calculated. In this respect it was shown that the linear approximation for the nuclear polarization generally used in calculations so far is not a good approximation for indium because of its large spin of $I = 9/2$. The full Brillouin function without approximations was used to calculate the nuclear field in the specific case of

a purely longitudinal external field.

It was found that neglecting losses the nuclear field at zero externally applied field is as high as ≈ 4 T, which is due to nuclear polarization under the exclusive influence of the Knight field. It was also calculated that the nuclear polarization could reach $> 95\%$ for a fully polarized electron spin, as the maximum Knight field values, ≈ 1.7 mT, dominates over the dipole-dipole field. This nuclear field, reaching up to 7.9 T provides an explanation of the observation of polaron formation at 2 K, as theoretically predicted [45] and for which experimental evidence already has been provided [23, 25].

Acknowledgments

This work was supported by the Deutsche Forschungsgemeinschaft (grant BA 1549/12-1) and the BMBF research program “Nanoquit”. S. Yu. Verbin and R. V. Cherbunin acknowledge support of the Russian Ministry of Science and Education (grant RNP.2.1.1.362) and the Russian Foundation for Basic Research, R. Oulton thanks the Alexander von Humboldt foundation.

-
- [*] e-mail: thomas.auer@e2.physik.uni-dortmund.de
- [†] Now: Department of Physics and Astronomy, The University of Sheffield, , Sheffield S3 7RH, United Kingdom. e-mail: r.oulton@sheffield.ac.uk
- [‡] Also in: I. A. Ioffe Physicotechnical Institute, Russian Academy of Science, 194021 Polytechnicheskaya 27, St. Petersburg, Russia
- [1] G. Lampel, Phys. Rev. Lett. **20**, 491 (1968).
- [2] A. I. Ekimov and V. I. Safarov, ZhETF Pis. Red. **15**, 257, 453 (1972) [JETP Lett. **15**, 179, 319 (1972)].
- [3] V. L. Berkovits, A. I. Ekimov, and V. I. Safarov, Zh. Eksp. Teor. Fiz. **65**, 346 (1973) [Sov. Phys. JETP **38**, 169 (1974)].
- [4] M. I. D'yakonov, V. I. Perel', V. L. Berkovits, and V. I. Safarov, Zh. Eksp. Teor. Fiz. **67**, 1912 (1974) [Sov. Phys. JETP **40**, 950 (1975)].
- [5] M. I. D'yakonov and V. I. Perel', Zh. Eksp. Teor. Fiz. **65**, 362 (1973) [Sov. Phys. JETP **38**, 177 (1974)].
- [6] V. A. Novikov and V. G. Fleisher, Pis'ma Zh. Tekh. Fiz. **20**, 935 (1975).
- [7] F. Meier and B. P. Zakharchenya (editors), *Optical Orientation*, Modern Problems in Condensed Matter Sciences, Vol. 8 (North-Holland, Amsterdam, 1984).
- [8] D. Paget, G. Lampel, B. Sapoval, and V. I. Safarov, Phys. Rev. B **15**, 5780 (1977).
- [9] I. A. Akimov, D. H. Feng, and F. Henneberger, Phys. Rev. Lett. **97**, 056602 (2006).
- [10] V. L. Berkovits, C. Hermann, G. Lampel, A. Nakamura, and V. I. Safarov, Phys. Rev. B **18**, 1767 (1978).
- [11] S. W. Brown, T. A. Kennedy, D. Gammon, and E. S. Snow, Phys. Rev. B **54**, 17339 (1996).
- [12] A. Imamoglu, E. Knill, L. Tian, and P. Zoller, Phys. Rev. Lett. **91**, 017402 (2003).
- [13] B. Eble, O. Krebs, A. Lematre, K. Kowalik, A. Kudelski, P. Voisin, B. Urbaszek, X. Marie, and T. Amand, Phys. Rev. B **74**, 081306 (2006).
- [14] A. I. Tartakovskii, T. Wright, A. Russell, V. I. Fal'ko, A. B. Van'kov, J. Skiba-Szymanska, I. Drouzas, I. R. S. Kolodka, M. S. Skolnick, P. W. Fry, A. Tahraoui, H.-Y. Liu, and M. Hopkinson, Phys. Rev. Lett. **98**, 026806 (2007).
- [15] P.-F. Braun, B. Urbaszek, T. Amand, X. Marie, O. Krebs, B. Eble, A. Lemaitre, and P. Voisin, Phys. Rev. B **74**, 245306 (2006).
- [16] A. W. Overhauser, Phys. Rev. **92**, 411 (1953).
- [17] D. H. Feng, I. A. Akimov, and F. Henneberger, Phys. Rev. Lett. **99**, 036604 (2007).
- [18] P. Maletinsky, A. Badolato, and A. Imamoglu, Phys. Rev. Lett. **99**, 056804 (2007).
- [19] C. W. Lai, P. Maletinsky, A. Badolato, and A. Imamoglu, Phys. Rev. Lett. **96**, 167403 (2006).
- [20] W. D. Knight, Phys. Rev. **76**, 1259 (1949).
- [21] I. A. Merkulov, Al. L. Efros, and M. Rosen, Phys. Rev. B **65**, 205309 (2002).
- [22] P.-F. Braun, X. Marie, L. Lombez, B. Urbaszek, T. Amand, P. Renucci, V. K. Kalevich, K. V. Kavokin, O. Krebs, P. Voisin, and Y. Masumoto, Phys. Rev. Lett. **94**, 116601 (2005).
- [23] R. Oulton, A. Greilich, S. Yu. Verbin, R. V. Cherbunin, T. Auer, D. R. Yakovlev, M. Bayer, I. A. Merkulov, V. Stavarache, D. Reuter, and A. D. Wieck, Phys. Rev. Lett. **98**, 107401 (2007).
- [24] D. Stepanenko, G. Burkard, G. Giedke, and A. Imamoglu, Phys. Rev. Lett. **96**, 136401 (2006).

- [25] R. Oulton, S. Yu. Verbin, T. Auer, R. V. Cherbunin, A. Greulich, D. R. Yakovlev, M. Bayer, D. Reuter, and A. Wieck, *Phys. Stat. Sol. (b)* **243**, 3922 (2006).
- [26] A. Greulich, R. Oulton, E. A. Zhukov, I. A. Yugova, D. R. Yakovlev, M. Bayer, A. Shabaev, Al. L. Efros, I. A. Merkulov, V. Stavarache, D. Reuter, and A. Wieck, *Phys. Rev. Lett.* **96**, 227401 (2006).
- [27] S. Cortez, O. Krebs, S. Laurent, M. Senes, X. Marie, P. Voisin, R. Ferreira, G. Bastard, J-M. Grard, and T. Amand, *Phys. Rev. Lett.* **89**, 207401 (2002).
- [28] S. Laurent, M. Senes, O. Krebs, V. K. Kalevich, B. Urbaszek, X. Marie, T. Amand, and P. Voisin, *Phys. Rev. B* **73**, 235302 (2006).
- [29] M. Ikezawa, B. Pal, Y. Masumoto, I. V. Ignatiev, S. Yu. Verbin, and I. Ya. Gerlovin, *Phys. Rev. B* **72**, 153302 (2005).
- [30] M. E. Ware, E. A. Stinaff, D. Gammon, M. F. Doty, A. S. Bracker, D. Gershoni, V. L. Korenev, S. C. Badescu, Y. Lyanda-Geller, and T. L. Reinecke, *Phys. Rev. Lett.* **95**, 177403 (2005).
- [31] Y. Masumoto, S. Oguchi, B. Pal, and M. Ikezawa, *Phys. Rev. B* **74**, 205332 (2006).
- [32] V. K. Kalevich, I. A. Merkulov, A. Yu. Shiryaev, K. V. Kavokin, M. Ikezawa, T. Okuno, P. N. Brunkov, A. E. Zhukov, V. M. Ustinov, and Y. Masumoto, *Phys. Rev. B* **72**, 045325 (2005).
- [33] M. Bayer, G. Ortner, O. Stern, A. Kuther, A. A. Gorbunov, A. Forchel, P. Hawrylak, S. Fafard, K. Hinzer, T. L. Reinecke, S. N. Walck, J. P. Reithmaier, F. Klopff, and F. Schfer, *Phys. Rev. B* **65**, 195315 (2002).
- [34] I. A. Akimov, K. V. Kavokin, A. Hundt, and F. Henneberger, *Phys. Rev. B* **71**, 075326 (2005).
- [35] A. V. Khaetskii and Y. V. Nazarov *Phys. Rev. B* **61**, 12639 (2000).
- [36] R. I. Dzhioev, B. P. Zakharchenya, V. L. Korenev, and M. V. Lazarev, *Phys. Solid State* **41**, 2014 (1999).
- [37] A. Abragam, *The Principles of Nuclear Magnetism*, (Clarendon Press, Oxford, 1983)
- [38] R. V. Cherbunin, I. V. Ignatiev, T. Auer, A. Greulich, R. Oulton, D. R. Yakovlev, M. Bayer, G. G. Kozlov, D. Reuter, and A. D. Wieck, submitted to *Phys. Rev. B*.
- [39] M. I. Dyakonov, and V. I. Perel, *Zh. Eksp. Teor. Fiz.* **68**, 1514 (1975).
- [40] M. Gueron, *Phys. Rev.* **135**, A200 (1964).
- [41] W. Hanle, *Z. Phys.* **30**, 93 (1924).
- [42] R. J. Epstein, D. T. Fuchs, W. V. Schoenfeld, P. M. Petroff, and D. D. Awschalom, *Appl. Phys. Lett.* **78**, 733 (2001).
- [43] A. S. Bracker, E. A. Stinaff, D. Gammon, M. E. Ware, J. G. Tischler, A. Shabaev, Al. L. Efros, D. Park, D. Gershoni, V. L. Korenev, and I. A. Merkulov, *Phys. Rev. Lett.* **94**, 047402 (2005)
- [44] J. Berezovsky, M. H. Mikkelsen, O. Gywat, N. G. Stoltz, L. A. Coldren, and D. D. Awschalom, *Science* **314**, 1916 (2006).
- [45] I. A. Merkulov, *Phys. of the Solid State* **40**, 930 (1998).